University of Kurdistan
Dept. of Electrical and Computer Engineering
Smart/Micro Grids Research Center
smgrc.uok.ac.ir

Modeling of Islanded Microgrids Using Static and Dynamic Equivalent Thevenin Circuits

Mobin Naderi, Yousef Khayat, Qobad Shafiee,
Hassan Bevrani, Frede Blaabjerg

Published in: Proceedings of the 20th European Conference on Power Electronics and Applications (EPE'18 ECCE Europe)

Modeling of Islanded Microgrids Using Static and Dynamic Equivalent Thevenin Circuits

Mobin Naderi, Yousef Khayat, Qobad Shafiee,
and Hassan Bevrani
Smart/Micro Grids Research Center,
University of Kurdistan,
Sanandaj P.C.: 66177-15175,
Kurdistan, Iran
m.naderi@eng.uok.ac.ir,y.khayat@eng.uok.ac.ir,
q.shafiee@uok.ac.ir, bevrani@uok.ac.ir

Frede Blaabjerg
Department of Energy Technology,
Aalborg University
Pontoppidanstræde 101, 9220 Aalborg Ø
Denmark
fbl@et.aau.dk

Keywords

« Device modeling », « Microgrid », «Voltage Source Inverters (VSI) », « Estimation technique ».

Abstract

In this paper, a new modeling method based on the equivalent Thevenin circuit is proposed for inverter-interfaced microgrids. The proposed method approximates the entire network connected to each inverter with an equivalent Thevenin circuit. The equivalent circuit is studied in two forms: static impedance and dynamic second-order RL branch. The static impedance equivalent circuit provides a good steady state but not a good transient response. To cope with this issue, the static impedance is replaced with a dynamic second-order RL branch, which results in appropriate transients. Both static and dynamic models are validated using a microgrid test system simulated in MATLAB/SimPowerSystems.

1. Introduction

A basic change in the production and consumption of the electricity energy is formed in the past two decades, and it is continuing. The electricity industry has tended to the modern power grids due to some characteristics of the conventional power systems including large losses, cost of long transmission lines and large power plants, environmental issues, and energy supply security and reliability [1]. To meet these challenges, new power grids, named smart grids, have been proposed which intelligently monitors, predicts, and controls the behaviors of electric power users and grid operation [2]. Although the modern grids can overcome most of the conventional power system issues, they create new challenges such as high penetration of distributed energy resources (DERs). Microgrid, which is a new concept for integration of DERs, is a good solution for the many of these challenges [3].

A microgrid is a new configuration of power systems composed of distributed energy resources and local loads, which can operate in both grid-connected and islanded modes [4]. In the islanded mode of operation, voltage and frequency regulation are the main control objectives. In fact, the stability analysis and controller design is an important issue in the islanded microgrids [5]-[7]. To provide such an analysis and design, a dynamic model of the system is essential. In this regard, many dynamic models have been introduced in the literature [8]-[9]. The existing works model all the microgrid components to design low level controllers of one DER. When this type of modeling is extended to the whole microgrid, a model with a large order may be derived [6], [9]. However, independent modeling

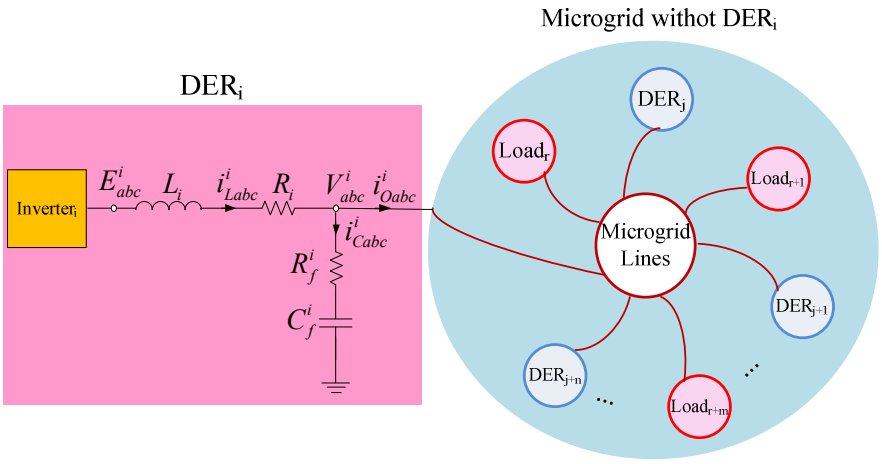

Fig. 1: General diagram of an islanded ac microgrid with focus on DER_i.

of a DER from the rest of the microgrid results in low model order and facilitates procedure of analysis and design.

In this paper, a new modeling approach based on the equivalent Thevenin circuit is proposed for microgrids. Unlike the existing approaches, each DER is modeled independently, while the rest of the microgrid components are taken into account using a simple equivalent Thevenin circuit. An equivalent Thevenin circuit is considered without dynamic, which ignores all dynamic effects of the rest of the microgrids on the corresponding inverter-based DER. A dynamic equivalent Thevenin circuit is then studied similar to a series resistance and inductance branch, to provide more accurate modeling of the DER.

2. Inverter modeling

Two different inverter modeling are conducted in this section: static modeling, and dynamic modeling. The static impedance Z_{th} (SIZ) model utilizes a Thevenin impedance without any dynamics, while the dynamic second-order RL (DSRL) includes two series RL and parallel RL branches.

2.1. Static Z_{th} Inverter Modeling

A conceptual diagram of an islanded microgrid in a general case is shown in Fig. 1 where the focus is on a single-line diagram of the DER_i. The DER_i is controlled as a voltage-source inverter and its DC-link voltage is assumed to be constant [10]. The rest of microgrid includes other DERs, loads, and lines, while they are electrically linked. The other DERs are operated in the form of voltage-source grid-supporting type [11]. Here, we aim to find a model for the DER_i distinct from the rest of microgrid. To achieve this goal, effects of the rest of microgrid on DER_i are considered in the form of an equivalent Thevenin circuit.

Fig. 2 shows the microgrid model consists of a voltage source representing the inverter, filter inductance, capacitance, resistances, and a Thevenin equivalent circuit. In the SIZ model, the Thevenin equivalent is composed of an impedance equivalent to all other impedances in the microgrid including lines, loads, and filters, and a voltage source equivalent to all other sources in the microgrid. In addition, two RL branches are considered instead of Z_{th} in the DSRL model to improve the transient performance. Three-phase equations in *abc*-frame are as follows

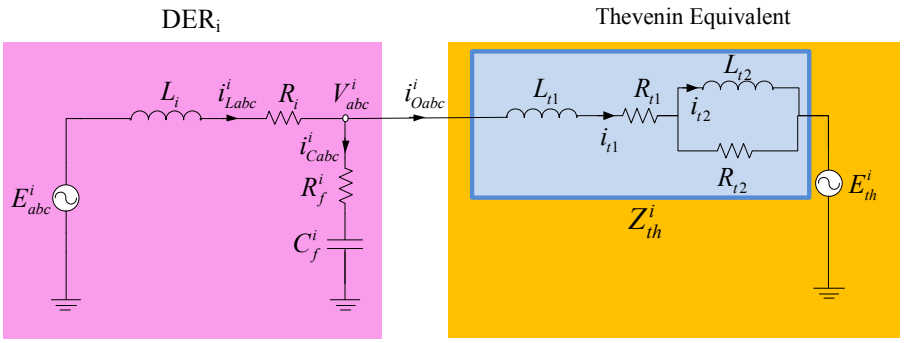

Fig. 2: The microgrid model focusing on DER$_i$ and Z^i_{th} modeled by two RL branches.

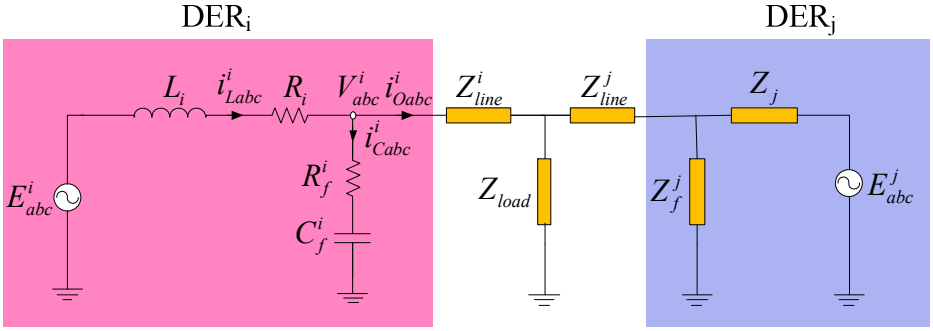

Fig. 3: A typical two-DER microgrid with lines and load.

$$E^i_{abc} = R_i i^i_{Labc} + L_i \frac{d}{dt} i^i_{Labc} + V^i_{abc} \tag{1}$$

$$i_{Cabc_i} = i_{Labc_i} - i_{Oabc_i} = C_{f_i} \frac{d}{dt} V_{abc_i} \tag{2}$$

$$V^i_{abc} = Z^i_{th} i^i_{Oabc} + E^i_{th} \tag{3}$$

where Z^i_{th} and E^i_{th} are calculated easily according to the structure of the rest of the microgrid. In the case of the two-DER microgrid shown in Fig. 3, Z^i_{th} and E^i_{th} are obtained as

$$\begin{cases} Z^i_{th} = Z^i_{line} + Z_{load} \,\|\, (Z^j_{line} + Z_j \,\|\, Z^j_f), \\ E^i_{th} = \left(\dfrac{(Z_j \,\|\, Z^j_f)(Z_{load} \,\|\, (Z^j_{line} + Z_j \,\|\, Z^j_f))}{Z_j (Z^j_{line} + Z_j \,\|\, Z^j_f)}\right) E^j_{an} \angle \varphi_j, \end{cases} \tag{4}$$

where E^j_{an} is the amplitude of phase voltage of the DER$_j$. By replacing (3) into (1) and (2), one can write

$$E^i_{abc} = R_i i^i_{Labc} + L_i \frac{d}{dt} i^i_{Labc} + Z^i_{th} i^i_{Oabc} + E^i_{th}, \tag{5}$$

$$C^i_f Z^i_{th} \frac{d}{dt} i^i_{Oabc} = i^i_{Labc} - i^i_{Oabc}. \tag{6}$$

Equations (5) and (6) are converted to the equivalent equations in *dq*-frame using Park and Clark transformations [12] as follows

$$C^i_f Z^i_{th,dq} \frac{d}{dt} i^i_{Odq} + j\omega C^i_f Z^i_{th,dq} i^i_{Odq} = i^i_{Ldq} - i^i_{Odq}, \tag{7}$$

$$E^i_{dq} = R_i i^i_{Ldq} + L_i \frac{d}{dt} i^i_{Ldq} + j\omega L_i i^i_{Ldq} + Z^i_{th} i^i_{Odq} + E^i_{th,dq}, \tag{8}$$

where $f_{dq}^i = f_d^i + jf_q^i$ and f can be all parameters and variables including E, E_{th}, i_L, i_O, and Z_{th}. By decoupling d and q axes, in order to derive a state space representation of the SIZ model with the states $X^i = [i_{Ld}^i \quad i_{Lq}^i \quad i_{Od}^i \quad i_{Oq}^i]^T$, control inputs $U^i = [E_d^i \quad E_q^i]^T$, and disturbance inputs $W^i = [E_{th,d}^i \quad E_{th,q}^i]^T$, (7) and (8) can be rewritten as

$$\begin{cases} \frac{d}{dt} i_{Ld}^i = -\frac{R_i}{L_i} i_{Ld}^i + \omega i_{Lq}^i - \frac{Z_{th,d}^i}{L_i} i_{Od}^i + \frac{Z_{th,q}^i}{L_i} i_{Oq}^i + \frac{1}{L_i} E_d^i - \frac{1}{L_i} E_{th,d}^i \\ \frac{d}{dt} i_{Lq}^i = -\omega i_{Ld}^i - \frac{R_i}{L_i} i_{Lq}^i - \frac{Z_{th,q}^i}{L_i} i_{Od}^i - \frac{Z_{th,d}^i}{L_i} i_{Oq}^i + \frac{1}{L_i} E_q^i - \frac{1}{L_i} E_{th,q}^i \\ \frac{d}{dt} i_{Od}^i = \frac{1}{K_{th,d}^i} i_{Ld}^i + \frac{1}{K_{th,q}^i} i_{Lq}^i - \frac{1}{K_{th,d}^i} i_{Od}^i + (\omega - \frac{1}{K_{th,q}^i}) i_{Oq}^i, \\ \frac{d}{dt} i_{Oq}^i = -\frac{1}{K_{th,q}^i} i_{Ld}^i + \frac{1}{K_{th,d}^i} i_{Lq}^i + (\frac{1}{K_{th,q}^i} - \omega) i_{Od}^i - \frac{1}{K_{th,d}^i} i_{Oq}^i, \end{cases} \tag{9}$$

where $K_{th,d}^i = \frac{C_f^i}{Z_{th,d}^i}(Z_{th,d}^{i\,2} + Z_{th,q}^{i\,2})$ and $K_{th,q}^i = \frac{C_f^i}{Z_{th,q}^i}(Z_{th,d}^{i\,2} + Z_{th,q}^{i\,2})$.

Since the aim is to control the output inverter current i.e. set of i_{Ld}^i and i_{Lq}^i, it is considered as the desired output. Thus, the differential equations (9) are expressed like a state space model as follows

$$\begin{cases} \frac{d}{dt} X^i = A^i X^i + B_1^i U^i + B_2^i W^i \\ Y^i = C^i X^i + D_1^i U^i + D_2^i W^i \end{cases} \tag{10}$$

where

$$A^i = \begin{bmatrix} -\frac{R_i}{L_i} & \omega & -\frac{Z_{th,d}^i}{L_i} & \frac{Z_{th,q}^i}{L_i} \\ -\omega & -\frac{R_i}{L_i} & -\frac{Z_{th,q}^i}{L_i} & -\frac{Z_{th,d}^i}{L_i} \\ \frac{1}{K_{th,d}^i} & \frac{1}{K_{th,q}^i} & -\frac{1}{K_{th,d}^i} & \omega - \frac{1}{K_{th,q}^i} \\ -\frac{1}{K_{th,q}^i} & \frac{1}{K_{th,d}^i} & \frac{1}{K_{th,q}^i} - \omega & -\frac{1}{K_{th,d}^i} \end{bmatrix} \quad B_1^i = \begin{bmatrix} \frac{1}{L_i} & 0 \\ 0 & \frac{1}{L_i} \\ 0 & 0 \\ 0 & 0 \end{bmatrix}, \quad B_2^i = \begin{bmatrix} -\frac{1}{L_i} & 0 \\ 0 & -\frac{1}{L_i} \\ 0 & 0 \\ 0 & 0 \end{bmatrix}.$$

To derive the output equations, (10) should be rewritten as

$$\frac{d}{dt}\begin{bmatrix} i_{Ldq}^i \\ i_{Odq}^i \end{bmatrix} = \begin{bmatrix} A_{11}^i & A_{12}^i \\ A_{21}^i & A_{22}^i \end{bmatrix}\begin{bmatrix} i_{Ldq}^i \\ i_{Odq}^i \end{bmatrix} + \begin{bmatrix} B_{L11}^i & B_{L12}^i \\ B_{O21}^i & B_{O22}^i \end{bmatrix}\begin{bmatrix} E_{dq}^i \\ E_{th,dq}^i \end{bmatrix}. \tag{11}$$

Where $i_{Ldq}^i = [i_{Ld}^i \quad i_{Lq}^i]^T$, $i_{Ldq,ref}^i = [i_{Ld,ref}^i \quad i_{Lq,ref}^i]^T$, $i_{Odq}^i = [i_{Od}^i \quad i_{Oq}^i]^T$, $E_{dq}^i = [E_d^i \quad E_q^i]^T$, $E_{th,dq}^i = [E_{th,d}^i \quad E_{th,q}^i]^T$, and

$$A_{11}^i = \begin{bmatrix} -\frac{R_i}{L_i} & \omega \\ -\omega & -\frac{R_i}{L_i} \end{bmatrix}, \quad A_{12}^i = \begin{bmatrix} -\frac{Z_{th,d}^i}{L_1} & \frac{Z_{th,q}^i}{L_1} \\ -\frac{Z_{th,q}^i}{L_1} & -\frac{Z_{th,d}^i}{L_1} \end{bmatrix}, \quad A_{21}^i = \begin{bmatrix} \frac{1}{K_{th,d}^i} & -\frac{1}{K_{th,q}^i} \\ \frac{1}{K_{th,q}^i} & \frac{1}{K_{th,d}^i} \end{bmatrix},$$

$$A_{22}^i = \begin{bmatrix} -\frac{1}{K_{th,d}^i} & \omega - \frac{1}{K_{th,q}^i} \\ \frac{1}{K_{th,q}^i} - \omega & -\frac{1}{K_{th,d}^i} \end{bmatrix}, \quad B_{L11}^i = \begin{bmatrix} \frac{1}{L_i} & 0 \\ 0 & \frac{1}{L_i} \end{bmatrix},$$

and $B^i_{L12} = -B^i_{L11}$, and $B^i_{O21} = B^i_{O22} = 0_{2\times 2}$. Thus, one can write

$$\frac{d}{dt} i^i_{Ldq} = A^i_{11} i^i_{Ldq} + A^i_{12} i^i_{Odq} + B^i_{L11} E^i_{dq} - B^i_{L11} E^i_{th,dq} . \tag{12}$$

According to Fig. 2, the output filter voltage is calculated as

$$V^i_{dq} = E^i_{dq} + M^i_{RL} i^i_{Ldq} + M^i_L \frac{d}{dt} i^i_{Ldq}, \tag{13}$$

where,

$$M^i_{RL} = \begin{bmatrix} -R_i & \omega L_i \\ -\omega L_i & -R_i \end{bmatrix}, \quad M^i_L = \begin{bmatrix} -L_i & 0 \\ 0 & -L_i \end{bmatrix}.$$

The derived model is called SIZ model due to its static Thevenin impedance. This model provides the stability analysis and design ability of a distinct voltage controller for any inverter in the microgrid by some control efforts on the output inverter voltage i.e. set of E^i_d and E^i_q. However, $E^i_{th,dq}$, the disturbance input, may affect the control procedure. Hence, disturbance attenuation may be included into the voltage controller design. Finally, by replacing (12) in (13) the output equation of (10) is obtained using matrices $C^i = \begin{bmatrix} M^i_{RL} + M^i_L A^i_{11} & M^i_L A^i_{12} \end{bmatrix}$, $D^i_1 = I_2 + M^i_L B^i_{L11}$, $D^i_2 = -M^i_L B^i_{L11}$.

2.2. Dynamic Second-order RL Inverter Modeling

The modeling procedure is repeated considering two series and parallel RL branches instead of Z^i_{th} as shown in Fig. 2. Using differential inductance equation on the right part of the model in Fig. 2 one can write

$$V^i_{abc} = R_{t1} i_{t1} + L_{t1} \frac{di_{t1}}{dt} + L \frac{di_{t1}}{dt} + E^i_{th}, \tag{14}$$

$$i_{t1} = \frac{L_{t2}}{R_{t2}} \frac{di_{t2}}{dt} + i_{t2} . \tag{15}$$

By replacing (15) in (14) and rewriting those in the state variable form and also using (5) and (6), the differential equations of the DSRL model is obtained as follows

$$\begin{cases} \frac{d}{dt} i^i_{Ld} = -\frac{R_i}{L_i} i^i_{Ld} + \omega i^i_{Lq} - \frac{1}{L_i} V^i_d + \frac{1}{L_i} E^i_d, \\ \frac{d}{dt} i^i_{Lq} = -\omega i^i_{Ld} - \frac{R_i}{L_i} i^i_{Lq} - \frac{1}{L_i} V^i_q + \frac{1}{L_i} E^i_q, \\ \frac{d}{dt} V^i_d = \frac{1}{C^i_f} i^i_{Ld} + \omega V^i_q - \frac{1}{C^i_f} i^i_{Od}, \\ \frac{d}{dt} V^i_q = \frac{1}{C^i_f} i^i_{Lq} - \omega V^i_d - \frac{1}{C^i_f} i^i_{Oq}, \\ \frac{d}{dt} i^i_{t1d} = \frac{1}{L^i_{t1}} V^i_d - \frac{R^i_{t1} + R^i_{t2}}{L^i_{t1}} i^i_{t1d} + \omega i^i_{t1q} + \frac{R^i_{t2}}{L^i_{t1}} i^i_{t2d} - \frac{1}{L^i_{t1}} E^i_{th,d}, \\ \frac{d}{dt} i^i_{t1q} = \frac{1}{L^i_{t1}} V^i_q - \omega i^i_{t1d} - \frac{R^i_{t1} + R^i_{t2}}{L^i_{t1}} i^i_{t1q} + \frac{R^i_{t2}}{L^i_{t1}} i^i_{t2q} - \frac{1}{L^i_{t1}} E^i_{th,q}, \\ \frac{d}{dt} i^i_{t2d} = \frac{R^i_{t2}}{L^i_{t2}} i^i_{t1d} - \frac{R^i_{t2}}{L^i_{t2}} i^i_{t2d} + \omega i^i_{t2q}, \\ \frac{d}{dt} i^i_{t2q} = \frac{R^i_{t2}}{L^i_{t2}} i^i_{t1q} - \omega i^i_{t2d} - \frac{R^i_{t2}}{L^i_{t2}} i^i_{t2q}. \end{cases} \tag{16}$$

Table I: Electrical parameters of the microgrid.

Parameters	Value	Parameters	Value
RMS Line-Line Voltage (V) and frequency (rad/s)	400, 100π	Shunt filter capacitance ($\left[C_f^1 \quad C_f^2\right]$) ($\mu F$)	$[20 \quad 20]$
Series filter resistance ($\left[R_1 \quad R_2\right]$) ($\Omega$)	$[0.3 \quad 0.3]$	Line impedance $\left[Z_{line}^1 \quad Z_{line}^2\right]^T$ (Ω)	$\begin{bmatrix}1.02+j1.005\\1.02+j1.005\end{bmatrix}$
Series filter inductance ($\left[L_1 \quad L_2\right]$) ($m$H)	$[5 \quad 7.1]$	Load impedance (Ω)	$1.898+j0.627$

Thus, to control the output filter current, the DSRL state space model can be represented by (10) with $X^i=[i_{Ld}^i \quad i_{Lq}^i \quad V_d^i \quad V_q^i \quad i_{t1d}^i \quad i_{t1q}^i \quad i_{t2d}^i \quad i_{t2q}^i]^T$, previous control and disturbance inputs and following matrices

$$A^i=\begin{bmatrix}
-\frac{R_i}{L_i} & \omega & -\frac{1}{L_i} & 0 & 0 & 0 & 0 & 0\\
-\omega & -\frac{R_i}{L_i} & 0 & -\frac{1}{L_i} & 0 & 0 & 0 & 0\\
\frac{1}{C_f^i} & 0 & 0 & \omega & -\frac{1}{C_f^i} & 0 & 0 & 0\\
0 & \frac{1}{C_f^i} & -\omega & 0 & 0 & -\frac{1}{C_f^i} & 0 & 0\\
0 & 0 & \frac{1}{L_{t1}^i} & 0 & -\frac{R_{t1}^i+R_{t2}^i}{L_{t1}^i} & \omega & \frac{R_{t2}^i}{L_{t1}^i} & 0\\
0 & 0 & 0 & \frac{1}{L_{t1}^i} & -\omega & -\frac{R_{t1}^i+R_{t2}^i}{L_{t1}^i} & 0 & \frac{R_{t2}^i}{L_{t1}^i}\\
0 & 0 & 0 & 0 & \frac{R_{t2}^i}{L_{t2}^i} & 0 & -\frac{R_{t2}^i}{L_{t2}^i} & \omega\\
0 & 0 & 0 & 0 & 0 & \frac{R_{t2}^i}{L_{t2}^i} & -\omega & -\frac{R_{t2}^i}{L_{t2}^i}
\end{bmatrix},$$

$$B_1^i=\begin{bmatrix}
\frac{1}{L_i} & 0 & 0 & 0 & 0 & 0 & 0 & 0\\
0 & \frac{1}{L_i} & 0 & 0 & 0 & 0 & 0 & 0
\end{bmatrix}^T,$$

$$B_2^i=\begin{bmatrix}
0 & 0 & 0 & 0 & 0 & 0 & -\frac{1}{L_{t1}^i} & 0\\
0 & 0 & 0 & 0 & 0 & 0 & 0 & -\frac{1}{L_{t1}^i}
\end{bmatrix}^T,$$

$$C^i=\begin{bmatrix}1 & 0 & 0 & 0 & 0 & 0 & 0 & 0\\ 0 & 1 & 0 & 0 & 0 & 0 & 0 & 0\end{bmatrix}.$$

3. Verification of the proposed model

In order to verify the proposed models, the typical two-DER microgrid, as shown in Fig. 3, with the parameters listed in Table I is simulated in the MATLAB/SimPowerSystems. This simulated system is compared with the two obtained models (SIZ and DSRL).

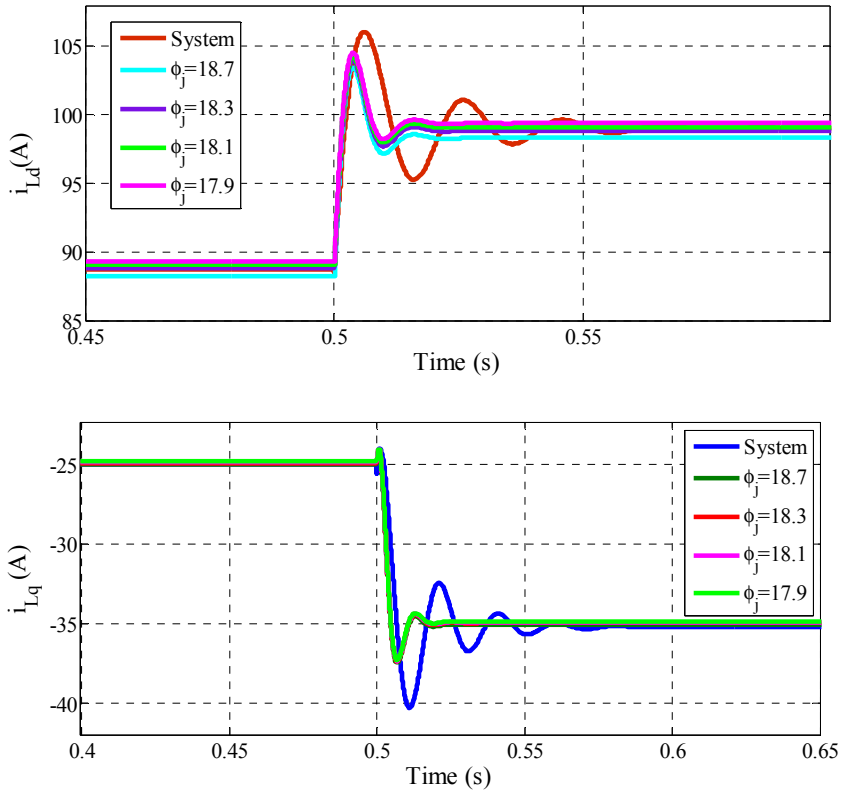

Fig. 4: Step responses of the inverter currents in the presence of DER_j voltage phase changes.

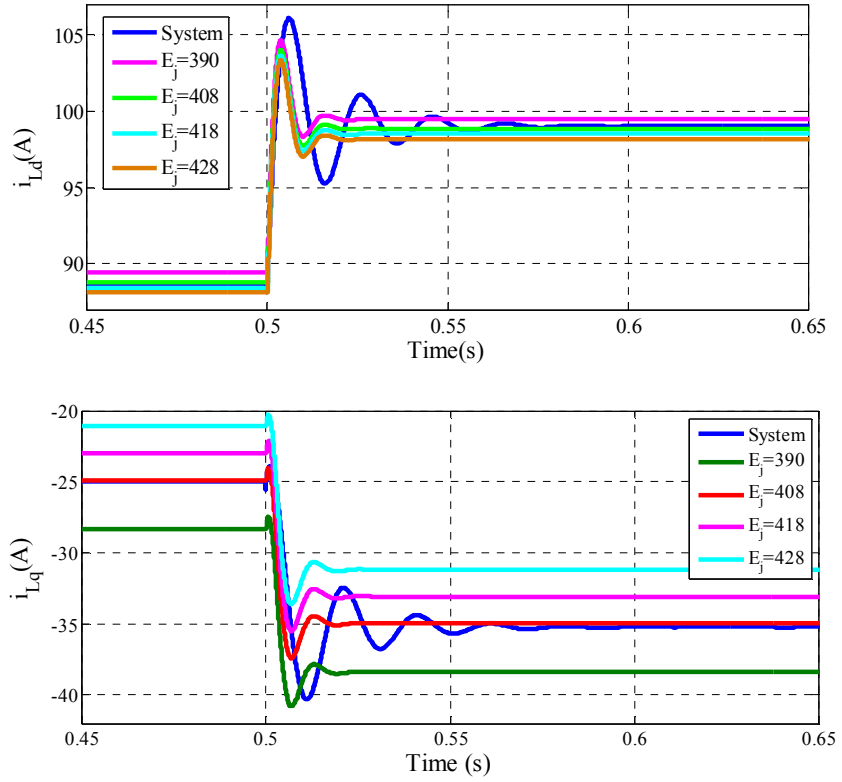

Fig. 5: Step responses of the inverter currents in the presence of DER_j voltage amplitude changes.

In the first scenario, the output inverter currents, i.e., i_{Ld}^{i} and i_{Lq}^{i} are compared with the output of the SIZ model in the presence of the most important parameters changes. The steady state precision of SIZ

model is related to the estimation of the Thevenin impedance and voltage values. These two depend on the uncertain and hard-estimated parameters consisting of the DER_j's voltage amplitude and phase i.e., E_{an}^{j}, and φ_j. The estimation error or uncertainty of each parameter can mitigate the model precision. The best estimations for E_{an}^{j}, and φ_j are 408 V and 18.1°, respectively according to simulated system voltage amounts. Fig. 4 and Fig. 5 show the effects of the parameter changes on the step responses of the inverter currents, i_{Ld}^{i} and i_{Lq}^{i}. In each case, the inverter voltage E_{an}^{i} changes from 408 V to 449 V at *t=0.5* s with the same input signal for the simulated system and the model. From a steady state's point of view, it can be concluded that the steady state error of the SIZ model is acceptable for suitable estimation of the interfered uncertain parameters. The SIZ model response is faster than the system response with less settling time, and overshoot/undershoot. The most important reason for the difference between the model and system transients is the lack of dynamics in the Thevenin impedance. In fact, dynamics of all loads, lines and filters belong to the rest of microgrid are neglected to simplify the model.

In the DSRL model, by contrast, the dynamics are included by RL branches. Once more, the inverter voltage E_{an}^{i} is changed from 408V to 449V at *t=0.5* s with the same input signal for the simulated system, SIZ and DSRL models. Fig. 6 shows the direct and quadratic components of the DER_1's filter current. Clearly, the transients are improved by considering four state variables for the equivalent Thevenin circuit. Overshoot and settling time are improved considerably by using DSRL modeling.

Another comparison is done in *abc* frame by increasing the load by 30% at *t=1* s and decreasing it at *t=1.5* s. A PI voltage controller is considered for both simulated inverter and its DSRL model. Current and voltage of the phase *a* can be seen in Fig. 7 during the load disturbances. According to Fig. 7, except a little difference in the transients, the DSRL model completely mimic the behavior of the system. Similar results can be shown for currents and voltages of the other two phases.

4. Conclusion

This paper proposes two new modeling approaches for islanded microgrids based on equivalent Thevenin circuit namely SIZ and DSRL models. The SIZ model with four states can well track the set point with a steady state error less than 1%, while having poor accuracy on transients. The DSRL model with eight states provides much better transients compared with the SIZ model. Indeed, both SIZ and DSRL models mimic the behavior of the system in the steady state properly. However, only the DSRL

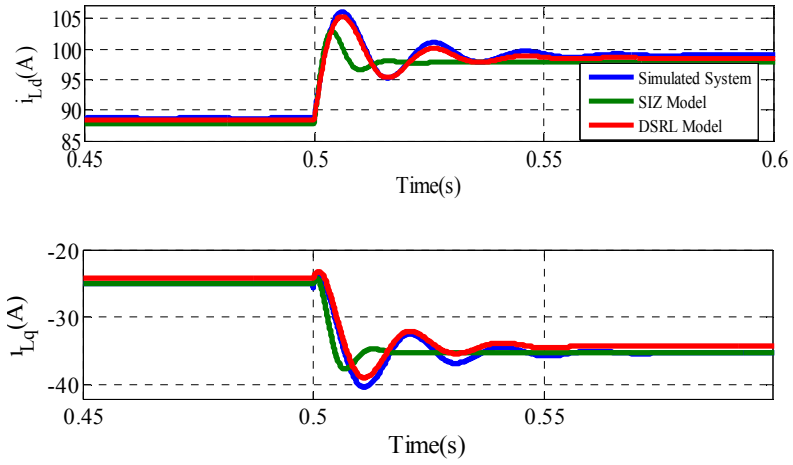

Fig. 6: Comparison study of the simulated system, SIZ, and DSRL models.

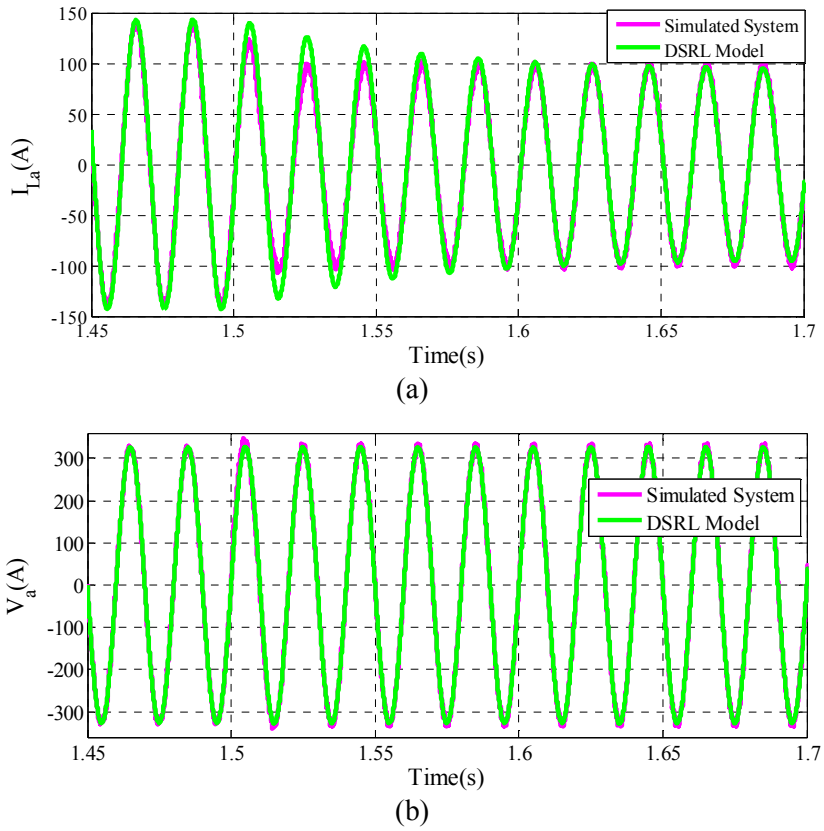

Fig. 7: Comparison between simulated system and DSRL model in *abc* frame: a) current of phase *a*, b) voltage of phase *a*.

model shows acceptable transient behavior. As a future work, more accurate models will be obtained by reasonable changing the connection type of resistances and inductances in the equivalent impedance.

References

[1] Bevrani H., Francois B., and Ise T.: Microgrid Dynamics and Control, John Wiley & Sons, 2017.

[2] Bevrani H., Masayuki W., Yasunori M.: Power system monitoring and control, John Wiley & Sons, 2014.

[3] Hatziargyriou N., Asano H., Iravani R., Marnay C., "Microgrids," *IEEE Power Energy Mag,.* vol. 5, no. 4, pp. 78-94, 2007.

[4] Wang X., Guerrero J. M., Chen Z.: Control of grid interactive AC microgrids, In Proc. *IEEE Int. Symp. Ind. Electron. (ISIE)* 2010, pp. 2211-2216.

[5] Guerrero J. M., Chandorkar M., Lee T. L., Loh P.C.: Advanced control architectures for intelligent microgrids—Part I: Decentralized and hierarchical control, *IEEE Trans. Ind. Electron.,* vol. 60, no. 4,pp. 1254-1262, Apr. 2013.

[6] Abdel-Rady M. Y., El-Saadany E. F.: Adaptive decentralized droop controller to preserve power sharing stability of paralleled inverters in distributed generation microgrids, *IEEE Trans. Power Electron.,* vol. 23, no. 6, pp. 2806-2816, 2008.

[7] Ashabani S. M., Abdel-Rady M. Y.: A flexible control strategy for grid-connected and islanded microgrids with enhanced stability using nonlinear microgrid stabilizer, *IEEE Trans. Smart Grid,* vol. 3, no. 3, pp. 1291-1301, 2012.

[8] Logenthiran T., Srinivasan D., Wong D.: Multi-agent coordination for DER in MicroGrid, *IEEE Int. Conf.* In *Sustain. Energy Tech.* 2008, pp. 77-82.

[9] Lenz E., Pagano D. J., Pou J.: Bifurcation analysis of parallel-connected voltage-source inverters with constant power loads, *IEEE Trans. Smart Grid*, to be published, 2017.

[10] Guerrero J. M., Matas J., De Vicuna L. G., Castilla M., Miret J.: Wireless-control strategy for parallel operation of distributed-generation inverters, *IEEE Trans. Ind. Electron.*, vol. 53, no. 5, pp. 1461–1470, 2006.

[11] Rocabert J., Luna A., Blaabjerg F., Rodriguez P.: Control of power converters in AC microgrids, *IEEE Trans. Power Electron.*, vol. *27* no. 11, pp. 4734-4749, 2012.

[12] Naderi M., Khayat Y., Batmani Y., Bevrani H.: Robust Multivariable Microgrid Control Synthesis and Analysis, *Energy Procedia,* vol. 100, 375-387, 2016.